

The physiologic aggresome mediates cellular inactivation of iNOS

Lavannya Pandit, Katarzyna E. Kolodziejska, Shenyan Zeng, and N. Tony Eissa¹

Department of Medicine, Baylor College of Medicine, Houston, TX 77030

Edited by Timothy Billiar, University of Pittsburgh Medical Center, Pittsburgh, PA, and accepted by the Editorial Board December 8, 2008 (received for review October 29, 2008)

Nitric Oxide (NO), produced by inducible nitric oxide synthase (iNOS), has been implicated in the pathogenesis of various biological and inflammatory disorders. Recent evidence suggests that aggresome formation is a physiologic stress response not limited to misfolded proteins. That stress response, termed “physiologic aggresome,” is exemplified by aggresome formation of iNOS, an important host defense protein. The functional significance of cellular formation of the iNOS aggresome is hitherto unknown. In this study, we used live cell imaging, fluorescence microscopy, and intracellular fluorescence NO probes to map the subcellular location of iNOS and NO under various conditions. We found that NO production colocalized with cytosolic iNOS but aggresomes containing iNOS were distinctly devoid of NO production. Further, cells expressing iNOS aggresomes produced significantly less NO as compared with cells not expressing aggresomes. Importantly, primary normal human bronchial epithelial cells, stimulated by cytokines to express iNOS, progressively sequestered iNOS to the aggresome, a process that correlated with marked reduction of NO production. These results suggest that bronchial epithelial cells used the physiologic aggresome mechanism for iNOS inactivation. Our studies reveal a novel cellular strategy to terminate NO production via formation of the iNOS aggresome.

misfolded | nitric oxide | primary cells | proteasome | degradation

Nitric oxide (NO), a multifunctional biological messenger, is synthesized from L-arginine by nitric oxide synthase (NOS) isoforms (1–3). As an agent of inflammation and cell-mediated immunity, NO is produced by a Ca²⁺-independent cytokine-inducible NOS (iNOS or NOSII) (2, 3). iNOS is distinct from the other constitutive NOS isoforms by its production of a relatively large amount of NO. It has been recognized that overproduction of NO by iNOS may cause tissue damage that outweighs its potential benefit for host defense (4). iNOS has been implicated in the pathogenesis of many inflammatory syndromes, e.g., asthma, transplant rejection, inflammatory bowel disease, rheumatoid arthritis, and septic shock (4, 5). Thus, understanding cellular processes responsible for controlling NO production by iNOS is critical for devising therapeutic strategies for inflammatory diseases associated with iNOS production.

Aggresomes are discrete cytoplasmic “inclusion bodies” that form in response to the production of misfolded proteins (6, 7). Aggresomes form around the microtubule-organizing center (MTOC) near the centrosome via dynein-directed retrograde transport of proteins on microtubule tracks. Recent evidence suggests that aggresome formation is also a physiologic mechanism to regulate certain cellular proteins. The latter process, termed “physiologic aggresome,” has been described in connection to cellular regulation of iNOS (8, 9). We have recently shown that iNOS is expressed initially as a cytosolic protein but is eventually targeted to a perinuclear location, identified by our data as an aggresome. Thus, the iNOS aggresome serves as a prototype for what we termed the physiologic aggresome. The term physiologic in this context is loosely used to describe aggresome formation which is not associated with known misfolded mutant proteins.

The above studies generated an important question: Does the aggresome mechanism represent a novel cellular mechanism for regulation of the activity of specific sets of proteins such as iNOS? Studies addressing these issues will have to overcome the technical hurdles of determining the target protein activity at various subcellular locations. In the case of iNOS, its enzymatic activity is associated with the production of NO. Therefore, with the recent development of molecular fluorescence probes to detect NO (10–13), we envisioned an opportunity to experimentally determine whether sequestration of iNOS to the aggresome serves as a means to regulate iNOS activity. In this study, we show that cellular sequestration of iNOS to the aggresome is associated with a loss of NO production by iNOS. Thus, our study reveals an important function of the physiologic aggresome in the inactivation of iNOS.

Results and Discussion

DAR-4M AM Is a Reliable Indicator of Subcellular NO Production by iNOS. DAR-4M AM, hereafter referred to as DAR, is a cell-permeable diamino-rhodamine-based dye that becomes fluorescent upon reacting with NO (10). To determine whether DAR could be reliably used as a marker for intracellular NO production by iNOS, we conducted several quality-control studies. HEK293 cells stably expressing iNOS-GFP were incubated in the presence of DAR and evaluated by live cell imaging. Parallel experiments were done using HEK293 cells not transfected with iNOS. In HEK293 cells not transfected with iNOS, fluorescence of DAR was not detected, reflecting lack of significant NO production in these cells (Fig. 1A) (14). In contrast, in HEK293 cells expressing iNOS-GFP, red fluorescence staining of DAR representing NO cellular location spatially corresponded to green fluorescence indicative of iNOS-GFP (Fig. 1B). Next, it was important to determine whether inhibition of NO production by iNOS-producing cells would correspondingly reduce fluorescence of DAR. We used the specific iNOS dimerization inhibitor BBS-2 to inhibit NO production by iNOS (15, 16). HEK293 cells, stably expressing iNOS-GFP and incubated with BBS-2, did not exhibit DAR fluorescence, reflecting the loss of NO production by iNOS in these cells (Fig. 1C). Finally, we demonstrated that we could restore DAR fluorescence in cells treated with iNOS inhibitor, using an NO donor (Fig. 1D). The diffuse presence of the dye represents the NO present in the system after addition of the NO donor to the media. These data demonstrate that DAR can be used as an effective marker of intracellular NO production by iNOS.

Author contributions: L.P., K.K., and N.T.E. designed research; L.P., K.K., and S.Z. performed research; L.P., K.K., and N.T.E. analyzed data; and L.P. and N.T.E. wrote the paper.

The authors declare no conflict of interest.

This article is a PNAS Direct Submission. T.B. is a guest editor invited by the Editorial Board.

¹To whom correspondence should be addressed. E-mail: teissa@bcm.edu.

This article contains supporting information online at www.pnas.org/cgi/content/full/0810968106/DCSupplemental.

© 2009 by The National Academy of Sciences of the USA

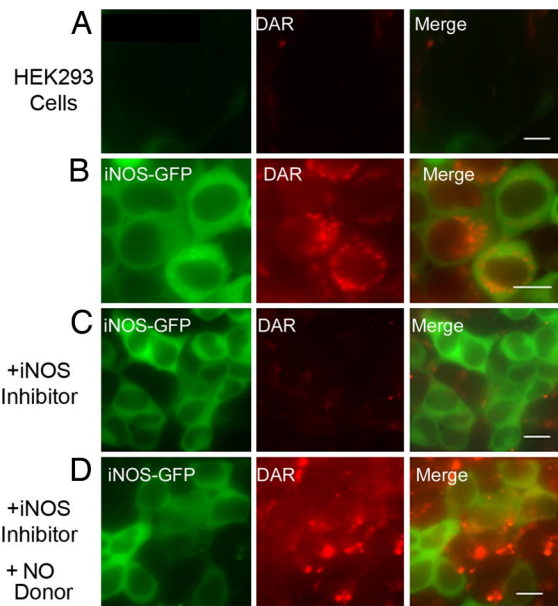


Fig. 1. Subcellular localization of iNOS and NO by live cell imaging. HEK293 cells were transfected for 18 h with plasmids encoding either a control vector encoding Lac-Z (A) or iNOS-GFP (B–D). After addition of DAR, live cell imaging was performed to assess the presence of iNOS-GFP (green) in relation to NO (red). Some experiments were done in the presence of the iNOS inhibitor BB5-2 (C). In D, cells from C were incubated with the NO donor SIN-1 (100 μ M) for 30 min. (Scale bar, 10 μ m.)

iNOS, Sequestered in Aggregates, Does Not Produce NO. We have previously shown that iNOS exists in 2 cellular compartments, the first being a diffuse cytosolic location and the second being a perinuclear compartment characterized as an iNOS aggregate, whose formation is accelerated by proteasomal inhibitors such as MG132 (8, 9). Using live cell imaging and DAR, we monitored the subcellular NO production over various time points in HEK293-iNOS-GFP cells in which iNOS aggregate formation was accelerated by the proteasome inhibitor MG132 (Fig. 2). At 1.5 h after the addition of MG132, the iNOS aggregate could be readily detected as a small perinuclear cluster at the MTOC but the majority of iNOS-GFP was still diffuse in the cytosol (Fig. 2A). The cytosolic iNOS-GFP corresponded to areas of fluorescent DAR, but there was a notable sparing of the DAR signals in the area occupied by the iNOS-GFP aggregate. This sparing of DAR fluorescence be-

came more evident as the size of the iNOS-GFP aggregate increased at later time points. At 18 h postproteasomal inhibition, most of the iNOS was concentrated in aggregates, while the cells became essentially devoid of DAR fluorescence. These data suggest that iNOS in the aggregates is inactive and thus does not produce detectable NO. To rule out the possibility that the lack of fluorescent DAR in the aggregate could be merely due to the aggregate representing a physical barrier for dye diffusion, we added the NO donor SIN-1 to the cells expressing iNOS aggregate. Using live cell imaging, we demonstrated that DAR fluorescence, reflecting NO generated from SIN-1, was readily detectable as diffuse staining in all areas of the cells, including the aggregate. (Fig. 2B). Thus, the aggregate is not a physical barrier to DAR uptake, and the sparing of DAR fluorescence in the aggregate (Fig. 2A) indicates that the iNOS aggregate serves as a depot of inactive iNOS.

The above data defined iNOS aggregate as functionally distinct from iNOS in the cytosol. To further confirm these observations, we designed experiments that would separate cells expressing predominantly cytosolic iNOS from cells expressing iNOS only in the aggregate. When cells are transfected with iNOS, because of variable levels of transfection in each cell, cells form iNOS aggregates at variable time points. Thus at any given time point following transfection there are 2 populations of cells. One group is composed of cells expressing diffuse cytosolic iNOS and the other group of cells already has iNOS sequestered in the aggregate. To separate the 2 populations, we capitalized on the observation that in cells expressing iNOS-GFP, the iNOS aggregate has a much higher fluorescence intensity compared to the remainder of the cell, likely due to the concentration of many iNOS-GFP molecules in a small compartment. Therefore, we used flow cytometry to sort HEK293 cells according to GFP fluorescence, 24 h following their transfection with iNOS-GFP (Fig. 3A). Cells with the lowest 70% GFP intensity were sorted as cells expressing cytosolic iNOS-GFP but not containing iNOS aggregates (X_1 cells in Fig. 3). Cells expressing the 10% highest GFP intensity were sorted as 1 population containing aggregates (X_2 cells in Fig. 3) with almost all these cells expressing iNOS aggregates. Cells not expressing detectable iNOS-GFP, i.e., nontransfected cells, were not further analyzed. In addition, cells expressing GFP fluorescence that lie in the middle 20% population of GFP intensity were not used to ensure complete separation between X_1 and X_2 cell populations. Fluorescence microscopy analysis of sorted cell populations confirmed that X_1 and X_2 cell populations expressed either cytosolic iNOS or iNOS aggregate, respectively (Fig. 3B). Equivalent numbers of each sorted cell population, X_1 and X_2 , were cultured

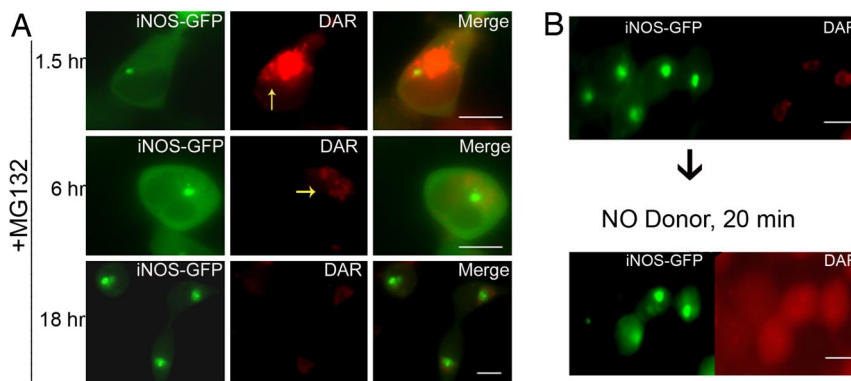


Fig. 2. iNOS in the aggregate does not produce NO. (A) Live cell imaging of HEK293 cells, stably expressing iNOS-GFP and incubated with DAR, was performed at various time points following the addition of 10 μ M of the proteasomal inhibitor MG132. Yellow arrows, in some panels, point to the site of aggregate formation being devoid of DAR fluorescence. (B) Experiments were done as in A except that addition of MG132 for 18 h was followed by the addition of the NO donor SIN-1 for 20 min. (Scale bar, 10 μ m.)

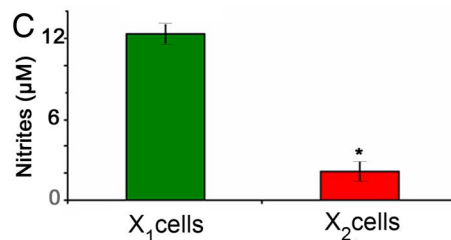
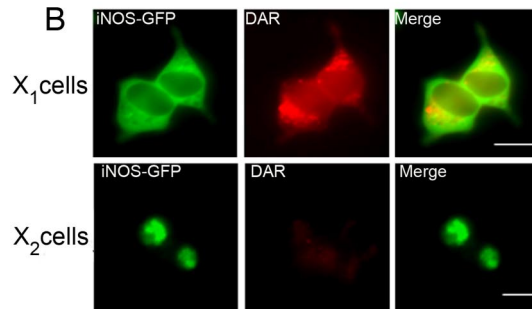
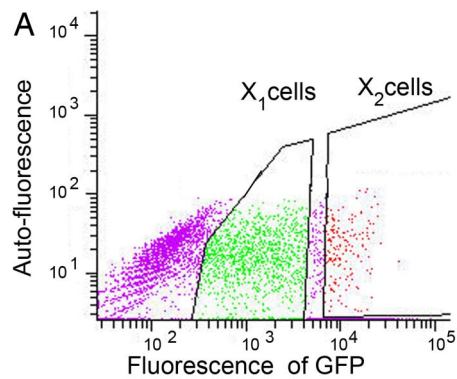


Fig. 3. Cells with iNOS aggresome produce less NO. HEK293 cells were transfected with iNOS-GFP. (A) Twenty-four hours following transfection, cells were sorted according to GFP intensity. Cells not likely to be transfected and thus exhibiting lowest fluorescence intensity were not further used. Cells expressing moderate and the top 10% of fluorescence intensity were termed X₁ and X₂, respectively. (B) Sorted cells were cultured for 24 h and then subjected to live cell imaging in the presence of DAR. Representative fluorescence microscopy images of sorted cells show marked enrichment of aggresome-containing cells in the X₂ population. (C) Nitrite accumulation in tissue culture media of sorted cells. *, $P < 0.05$. (Scale bar, 10 µm.)

for 24 h. NO production by iNOS was evaluated by live cell imaging using DAR and by measuring nitrite accumulation in culture media. Addition of DAR to each population reflected a significant lack of DAR fluorescence in the cells with aggresomes (X₂ cells) compared to diffuse DAR fluorescence in the cells without aggresomes (X₁ cells) (Fig. 3B). Furthermore, nitrite accumulation was significantly reduced in cells with aggresomes (X₂ cells) (Fig. 3C). These data suggest that iNOS sequestered to the aggresome does not produce detectable amounts of NO.

Lack of NO in Aggresomes Formed by Cytokine-Induced iNOS. In vivo, iNOS is expressed in states of inflammation and in response to proinflammatory cytokines (5, 17). We have previously shown that cytokine-induced iNOS is targeted to the aggresome in various human and murine cell lines (8). In RT4 cells, an epithelial cell line in which iNOS production and iNOS aggresomes have been well characterized (16, 18, 19), iNOS aggresome formation becomes clearly evident 24 h following cytokine stimulation (8). We investigated whether aggresomes formed by

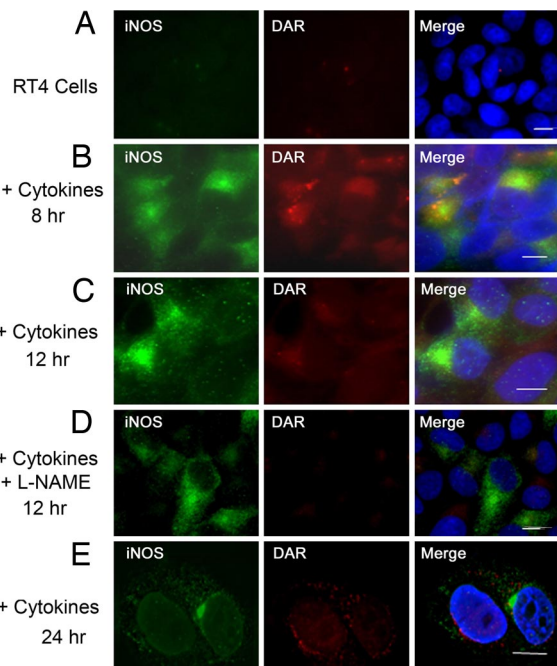


Fig. 4. Lack of NO in aggresomes of cytokine-induced iNOS. For induction of iNOS, RT4 cells were incubated, for various time points, in the presence or absence of a cytokine mixture of IFN- γ (100 units/ml), IL-1 β (0.5 ng/ml), and TNF- α (10 ng/ml). In D, the NOS inhibitor L-NAME was added to culture media. Following cytokine stimulation, cells were incubated for 1 h in the presence of DAR. Cells were then fixed, stained with 4',6-diamidino-2-phenylindole dihydrochloride (DAPI) to visualize nuclei (blue), and immunolabeled using an iNOS antibody and a goat anti-mouse conjugated to Alexa 488 (green). (Scale bar, 10 µm.)

cytokine-induced iNOS would contain inactive iNOS. RT4 cells were stimulated with a cytokine mixture of IFN- γ , IL-1 β , and TNF- α for various time points. Cells were then incubated for 1 h in the presence of DAR before they were fixed, immunostained with iNOS antibody, and evaluated by fluorescence microscopy. This strategy allowed us to examine subcellular localization of both NO, detected by fluorescent DAR, and iNOS, detected by immunofluorescence with iNOS antibody (Fig. 4). In the absence of cytokine stimulation, RT4 cells did not express any iNOS and there was no detectable DAR fluorescence, confirming a lack of NO production (Fig. 4A). At 8–12 h following cytokine stimulation, both iNOS and NO were mostly cytosolic (Fig. 4B and C). Parallel experiments were conducted in which RT4 cells were stimulated by the cytokine mixture for 12 h in the presence of NOS inhibitor L-NAME (2, 19). As expected, L-NAME inhibited NO production by iNOS and there was no detectable DAR fluorescence, further validating the use of DAR in this cellular model (Fig. 4D). In RT4 cells treated with cytokines for 24 h, iNOS was mostly sequestered in the perinuclear aggresome that was devoid of DAR fluorescence (Fig. 4E). These data suggest that the iNOS aggresome does not produce NO and are consistent with data shown above for transfected iNOS.

Primary Normal Human Bronchial Epithelial Cells Form Aggresomes That Sequester Inactive iNOS. We have previously shown that cytokine-induced iNOS is sequestered in a perinuclear aggresome in various human and murine cell lines (8, 9). Airway bronchial epithelial cells represent a major source of iNOS in the lung (17, 20). Alterations in iNOS levels in these cells have been implicated in the pathogenesis of several lung diseases such as asthma and cystic fibrosis (5, 21). We investigated whether iNOS

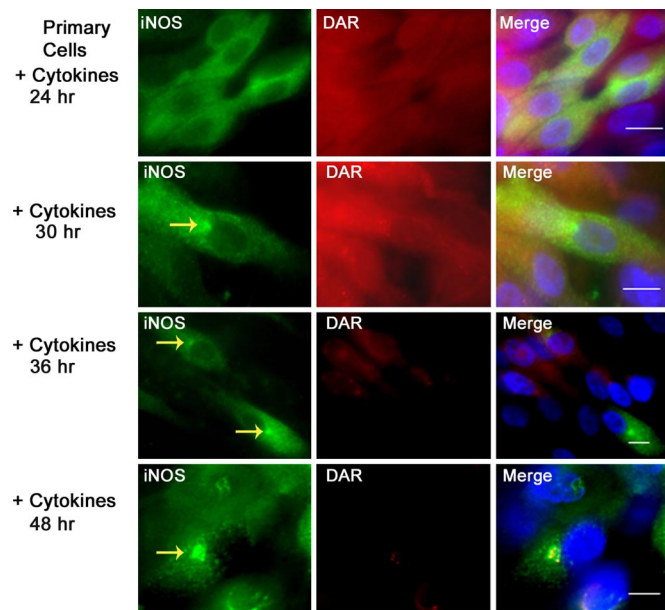


Fig. 5. iNOS aggresomes in primary normal human bronchial epithelial (NHBE) cells. Primary NHBE cells were grown to full differentiation at the air/liquid interface and stimulated with a cytokine mixture, as in Fig. 4, to induce iNOS expression. At various time points following cytokine stimulation, cells were incubated in the presence of DAR for 1 h. Cells were then fixed, stained with DAPI to visualize nuclei (blue), and immunolabeled using iNOS antibody (green). Yellow arrows, in *Left* panels, point to iNOS aggresomes. (Scale bar, 10 μ m.)

in primary normal human bronchial epithelial (NHBE) cells forms aggresomes and, if so, whether iNOS in the aggresomes is active. We cultured primary NHBE cells to full differentiation at the air/liquid interface (16, 19). These cells represent a closer model for the *in vivo* state in the lung airways. More importantly, when primary NHBE cells are cultured in the air/liquid interface they can achieve a state of differentiation that cannot otherwise be obtained in transformed cell lines or in primary cells cultured, submerged in culture medium (16, 19, 22). Primary NHBE cells were stimulated with cytokines for 24–48 h, incubated with DAR for 1 h, fixed, and immunoassayed with iNOS antibody (Fig. 5). Sequestration of iNOS to perinuclear aggresome became evident 30 h following cytokine stimulation and the aggresomes continued to increase in size at 36 and 48 h of cytokine addition. Monitoring both iNOS and NO in these cells revealed a progressive loss of NO production as revealed by diminished DAR and a corresponding increased iNOS sequestration to the aggresomes. In cells stimulated by cytokines for 48 h, despite abundant iNOS expression that was mostly in aggresomes, there was very little DAR fluorescence, reflecting lack of NO production. Serial analysis of NO production by iNOS, done by measuring nitrite in culture media, confirmed the progressive reduction in iNOS activity over time (data not shown). These data suggest that, in primary NHBE cells, the aggresome formation serves to inactivate iNOS.

To confirm that the iNOS aggresome in primary NHBE cells is a bona fide aggresome, we conducted several characterization studies. Similar to what was previously described for aggresomes, the iNOS aggresome in NHBE cells was formed at the MTOC, surrounded the centrosome, and was distinct from other perinuclear structures such as the Golgi (supporting information (SI) Fig. S1) (7–9).

Traditionally, aggresome formation is considered a cellular response to the aggregation of misfolded proteins (6, 7, 23). Recent work extends these observations to functional proteins

such as iNOS (8, 9). The functional significance of the latter observation is revealed by this study. Thus, what we term physiologic aggresome is a novel cellular mechanism to regulate the activity of certain proteins such as iNOS, an important host defense protein. The physiologic aggresome represents a stress-induced response that enables the cell to rapidly sequester a specific protein in a subcellular location for later disposal. This mechanism allows for the rapid inactivation of target proteins and thus adds a new dimension in cellular regulation of proteins.

A related question to the above findings would be whether a cellular aggresome substrate protein, such as iNOS, is inactivated by the aggresome or simply whether inactive iNOS accumulates in the aggresome. Our data demonstrate that iNOS located in the aggresome is inactive. Whereas the actual subcellular site where iNOS first loses its activity might be uncertain, iNOS inactivation is done in concert with its targeting to the aggresome. Thus, it is the overall cellular mechanism generating the aggresome pathway that is responsible for iNOS inactivation and sequestration. As has been previously shown, the aggresome pathway begins at various subcellular localizations where aggresome substrates interact with and are loaded onto the dynein motor for transport to the aggresome (7, 23). The loading for ubiquitinated substrates is facilitated by histone deacetylase 6 (HDAC6) that acts as an adaptor with binding domains for polyubiquitin chains and the dynein motor (6). In this context, it is important to note that our recent studies demonstrate that iNOS targeting to the aggresome pathway is dependent on the carboxy terminus of Hsp70-interacting protein (CHIP). CHIP targets iNOS to the aggresome by mediating its ubiquitination and facilitating iNOS interaction with HDAC6 (9).

It is interesting to note that in some cells expressing iNOS aggresomes, these cells displayed diffuse cytoplasmic iNOS but showed reduced NO production even outside the aggresome, for instance, in HEK293 cells following 6 h of postproteasomal inhibition (Fig. 2*A*, *Middle* row). This observation was also evident in primary NHBE cells at 48 h postcytokine stimulation (Fig. 5). These observations probably reflect the early stages of targeting iNOS to the aggresome, which include iNOS ubiquitination and its interactions with CHIP and HDAC6, as recently described (9). They also suggest that inactivation of iNOS by the aggresome pathway is likely to take place prior to iNOS final sequestration to the aggresome.

Critical review of several recent studies provides evidence that the physiologic aggresome mechanism might not be unique to iNOS. These studies describe cellular regulation of several important pathways through targeting key regulators, either for degradation or inactivation, to a perinuclear location at or near the centrosome at the MTOC, the site of aggresome formation. The regulation of cytokine signaling is critical for controlling cellular proliferation and activation during an immune response. Suppressor of cytokine signaling-1 (SOCS1) is a potent inhibitor of Jak kinase activity and of signaling initiated by several cytokines. Vuong *et al.* have shown that SOCS-1 is targeted to a perinuclear location near the MTOC where it is associated with the proteasome for potential degradation (24). Further, SOCS-1 targets Jak1 in an SH2-dependent manner to the same perinuclear location. Importantly, this process is dependent on the minus-end microtubule transport to the MTOC, a similar transport process shown for iNOS aggresome formation. Inhibition of this transport by nocadazole, a microtubule depolymerizing agent, led to elevated cellular levels of SOCS1 (24). These results suggest that both SOCS1 and Jak1, which are functional and not misfolded proteins, are regulated by the aggresome. Another signaling pathway that seems to be regulated by the aggresome is the bone morphogenic protein (BMP)/Smad1 signaling pathway. BMP receptors determine the intensity of BMP signals via Smad1 C-terminal phosphorylations. A recent study shows that a finely controlled cell biological pathway terminates this activity

by targeting activated Smad1 to the centrosome for degradation. The duration of the activated Smad1 signal is regulated by sequential Smad1 linker region phosphorylations at conserved MAPK and GSK3 sites required for its polyubiquitinylation and transport to the centrosome localization. Proteasomal degradation of activated Smad1 then takes place near the centrosome (25). Thus, the perinuclear aggresome serves as a depot for inactive Smad1 and eventual degradation.

Our study shows that the iNOS aggresome is an active participant in the cellular regulation of iNOS and that the cellular machinery promotes the formation of the iNOS aggresome as a physiologic response to stress in inflammation. These data are crucial to extending our knowledge on how cells respond in the pathogenesis of degenerative and inflammatory diseases.

Materials and Methods

Reagents and Antibodies. DAR-4M AM was purchased from Calbiochem. *N*-carbobenzoyl-L-leucyl-L-leucyl-L-norleucinal (MG132) SIN-1 (NO donor) was purchased from Sigma. iNOS dimerization inhibitor BBS-2 was kindly provided by Pfizer. iNOS antibody was from Research and Diagnostic Antibodies. Giantin, mouse monoclonal antibody (Abcam), and γ -tubulin mouse monoclonal antibody (Sigma) were used for Golgi and centrosome localization, respectively.

Cell Culture. HEK293 cells were cultured in improved MEM, and human bladder transitional cell papilloma (RT4) cells were cultured in McCoy's medium. Each medium was supplemented with 2 mM glutamine and 10% heat-inactivated FBS. All cells were maintained at 37 °C in 5% CO₂. Normal primary human bronchial epithelial cells (Lonza) were cultured in bronchial epithelial cell growth medium (BEGM, Lonza) containing 130 ng/ml bovine pituitary extract, 5×10^{-8} M retinoic acid, 1.5 μ g/ml BSA, 20 IU/ml nystatin, 0.5 mg/ml hydrocortisone, 25 ng/ml hEGF, 0.5 μ g/ml epinephrine, 10 μ g/ml transferrin, 5 μ g/ml insulin, 6.5 ng/ml triiodothyronine, and gentamicin (50 μ g/ml). Passage-2 cells were cultured at the air/liquid interface onto semipermeable membrane inserts (Transwell-clear; Corning) in a serum-free, 1:1 mixture of DMEM (Invitrogen) and BEGM supplemented as above. The cultures were grown submerged until cells reached 70% confluence. Thereafter, culture media were changed daily by replacing fresh media only to the basal compartment. After confluence, cultures were maintained at 37 °C in a humidified 5% CO₂ for 2 weeks until they reached a fully differentiated mucociliary

plateau phase. For iNOS induction, RT4 cells and differentiated normal primary human bronchial epithelial cells were stimulated by a mixture of IFN- γ (100 units/ml), IL-1 β (0.5 ng/ml), and TNF- α (10 ng/ml) (8, 16).

Plasmids and Transfections. Vectors encoding full-length iNOS cDNA or iNOS-GFP fusion protein were previously described (8, 26). Cationic lipid-mediated transient transfection was done using Lipofectamine 2000 (Invitrogen) following the manufacturer's instructions. All experiments on HEK-293 cells were done 24 h after transfection with iNOS-GFP fusion protein.

Immunofluorescence. Cells were grown on glass coverslips coated with poly(D)-lysine. Before fixation, cells were treated with DAR at 5 μ M concentration and maintained at 37 °C in 5% CO₂ for 1 h, followed by washing with 1 \times PBS for 10 min. Cells were then fixed in 4% paraformaldehyde, permeabilized by 0.2% Triton X-100, and blocked in 10% normal goat serum. Primary antibody incubation was done at room temperature for 1 h followed by a 30-min incubation at room temperature with Alexa fluor 594-labeled secondary antibodies (Molecular Probes). Coverslips were mounted by SlowFade gold antifade reagent with DAPI (Molecular Probes) and viewed by using a Zeiss Axiovert microscope deconvolution microscopy system. Imaging was performed using a Zeiss 63 \times (1.4 numerical aperture) oil immersion lens, and Z sections were collected at an optical depth of 0.25 μ m. Images were optimized by using Zeiss deconvolution software (8).

Live Cell Imaging. Cells, grown on black 0.17-mm Delta-T culture dishes (Bioptechs) at 37 °C in 5% CO₂, were treated with 5 μ M DAR for 1 h at 37 °C, followed by washing with PBS for 10 min. Dishes were then placed on a 37 °C temperature-controlled stage adaptor (Bioptechs) and viewed by using a Zeiss Axiovert microscope deconvolution microscopy system. Imaging was performed using a Zeiss 63 \times (1.4 numerical aperture) oil immersion lens, temperature controlled to 37 °C using an objective controller (Bioptechs).

Flow Cytometry. HEK293 cells, transiently transfected with iNOS-GFP, were sorted on the basis of GFP intensity using gates set to separate the highest 10% GFP fluorescent cells from the lowermost 70% GFP fluorescent cells. To ensure an adequate number of cells in each population, 100,000 events were counted.

ACKNOWLEDGMENTS. We thank Drs. Margie Moczygema and Li-Yuan Yu-Lee for useful discussions and critical review of the manuscript. We thank Pfizer for providing BBS-2. This work was supported by the National Heart Lung and Blood Institute, the National Institute of Allergy and Infectious Diseases, the American Heart Association, and the American Thoracic Society.

- Ignarro LJ, Buga GM, Wood KS, Byrns RE, Chaudhuri G (1987) Endothelium-derived relaxing factor produced and released from artery and vein is nitric oxide. *Proc Natl Acad Sci USA* 84:9265–9269.
- Stuehr DJ (1999) Mammalian nitric oxide synthases. *Biochim Biophys Acta* 1411:217–230.
- Xie, Q-w, et al. (1992) Cloning and characterization of inducible nitric oxide synthase from mouse macrophages. *Science* 256:225–228.
- Nathan C (1997) Inducible nitric oxide synthase: What difference does it make? *J Clin Invest* 100:2417–2423.
- Guo FH, et al. (2000) Molecular mechanisms of increased nitric oxide (NO) in asthma: evidence for transcriptional and post-translational regulation of NO synthesis. *J Immunol* 164:5970–5980.
- Kawaguchi Y, et al. (2003) The deacetylase HDAC6 regulates aggresome formation and cell viability in response to misfolded protein stress. *Cell* 115:727–738.
- Johnston JA, Ward CL, Kopito RR (1998) Aggresomes: a cellular response to misfolded proteins. *J Cell Biol* 143:1883–1898.
- Kolodziejka KE, Burns AR, Moore RH, Stenoien DL, Eissa NT (2005) Regulation of inducible nitric oxide synthase by aggresome formation. *Proc Natl Acad Sci USA* 102:4854–4859.
- Sha Y, Pandit L, Zeng S, Eissa NT (2009) A Critical Role for CHIP in the Aggresome Pathway. *Mol Cell Biol* 29:116–128.
- Kojima H, et al. (2001) Bioimaging of nitric oxide with fluorescent indicators based on the rhodamine chromophore. *Anal Chem* 73:1967–1973.
- von Bohlen und Halbach O, Albrecht D, Heinemann U, Schuchmann S (2002) Spatial nitric oxide imaging using 1,2-diaminoanthraquinone to investigate the involvement of nitric oxide in long-term potentiation in rat brain slices. *Neuroimage* 15:633–639.
- Brown LA, Key BJ, Lovick TA (1999) Bio-imaging of nitric oxide-producing neurons in slices of rat brain using 4,5-diaminofluorescein. *J Neurosci Methods* 92:101–110.
- Takata N, Harada T, Rose JA, Kawato S (2005) Spatiotemporal analysis of NO production upon NMDA and tetanic stimulation of the hippocampus. *Hippocampus* 15:427–440.
- Eissa NT, Yuan J, Haggerty CM, Choo EK, Moss J (1998) Cloning and characterization of human inducible nitric oxide synthase splice variants: a domain, encoded by exons 8 and 9, is critical for dimerization. *Proc Natl Acad Sci USA* 95:7625–7630.
- Enkhbaatar P, et al. (2003) The inducible nitric oxide synthase inhibitor BBS-2 prevents acute lung injury in sheep after burn and smoke inhalation injury. *Am J Respir Crit Care Med* 167:1021–1026.
- Kolodziejki PJ, Koo JS, Eissa NT (2004) Regulation of inducible nitric oxide synthase by rapid cellular turnover and cotranslational down-regulation by dimerization inhibitors. *Proc Natl Acad Sci USA* 101:18141–18146.
- Eissa NT, et al. (1996) Alternative splicing of human inducible nitric-oxide synthase mRNA: tissue-specific regulation and induction by cytokines. *J Biol Chem* 271:27184–27187.
- Kolodziejki PJ, Rashid MB, Eissa NT (2003) Intracellular formation of “undisruptable” dimers of inducible nitric oxide synthase. *Proc Natl Acad Sci USA* 100:14263–14268.
- Kolodziejki PJ, Musial A, Koo JS, Eissa NT (2002) Ubiquitination of inducible nitric oxide synthase is required for its degradation. *Proc Natl Acad Sci USA* 99:12315–12320.
- Guo FH, et al. (1995) Continuous nitric oxide synthesis by inducible nitric oxide synthase in normal human airway epithelium *in vivo*. *Proc Natl Acad Sci USA* 92:7809–7813.
- Zheng S, et al. (2003) Impaired innate host defense causes susceptibility to respiratory virus infections in cystic fibrosis. *Immunity* 18:619–630.
- Adler KB, Li Y (2001) Airway epithelium and mucus: intracellular signaling pathways for gene expression and secretion. *Am J Respir Cell Mol Biol* 25:397–400.
- Garcia-Mata R, Bebek Z, Sorscher EJ, Sztul ES (1999) Characterization and dynamics of aggresome formation by a cytosolic GFP-chimera. *J Cell Biol* 146:1239–1254.
- Vuong BQ, et al. (2004) SOCS-1 localizes to the microtubule organizing complex-associated 20S proteasome. *Mol Cell Biol* 24:9092–9101.
- Fuentealba LC, et al. (2007) Integrating patterning signals: Wnt/GSK3 regulates the duration of the BMP/Smad1 signal. *Cell* 131:980–993.
- Musial A, Eissa NT (2002) Inducible nitric oxide synthase is regulated by the proteasome degradation pathway. *J Biol Chem* 276:24268–24273.